

**PROBING TOP-QUARK COUPLINGS AT LEPTON AND PHOTON
COLLIDERS ***JOANNE L. HEWETT [†]
*Stanford Linear Accelerator Center,
Stanford University, Stanford, CA 94309, USA*

The ability of high energy lepton and photon colliders to probe the gauge couplings of the top-quark is summarized.

1. Introduction

The Standard Model (SM) has provided a remarkably successful description of almost all available data involving the strong and electroweak interactions. In particular, the discovery of the top-quark at the Tevatron with a mass¹ $m_t = 173.5 \pm 5.2$ GeV, close to that anticipated by fits to precision electroweak data² is a great triumph. Nonetheless, the SM leaves many fundamental questions unanswered, and this has led to numerous speculations on possible manifestations of new physics. Since the top-quark is the most massive fermion in the SM, it may provide a unique insight to new interactions originating at a higher scale. In fact, the detailed physics of the top-quark may be significantly different from what is predicted by the SM, making precision measurements of all its properties mandatory.

One possible manifestation of new interactions in the top-quark sector is to alter its couplings to the SM gauge bosons, W , Z , γ , or g . This possibility, extended to all of the fermions of the third generation, has attracted much attention³ in the recent literature. The most general gauge invariant, non-renormalizable three-point $t\bar{t}\gamma$, Z , g interactions can be written as

$$\mathcal{L} = g_V \bar{t} \left[\gamma_\mu (f_1^V + f_3^V \gamma_5) + \frac{i\sigma_{\mu\nu} q^\nu}{2m_t} (f_2^V + f_4^V \gamma_5) \right] t V^\mu, \quad (1)$$

where $g_\gamma = e$, $g_Z = g/2c_w$, and $g_g = g_s T_a$ for $V^\mu = A^\mu$, Z^μ , and $G^{a\mu}$, respectively, and q^ν corresponds to the momentum carried by the gauge boson. In the SM,

$$\begin{aligned} f_1^\gamma &= Q_t, & f_3^\gamma &= 0, \\ f_1^Z &= v_t, & f_3^Z &= a_t, \\ f_1^g &= 1, & f_3^g &= 0, \end{aligned} \quad (2)$$

^{*}To appear in the *Proceedings of the 2nd International Workshop on e^-e^- Interactions at TeV Energies*, Santa Cruz, CA, 22-24 September 1997

[†]Work supported by the Department of Energy, Contract DE-AC03-76SF00515

with Q_t, v_t, a_t being the top-quark's electric charge, and vector, axial-vector couplings to the Z . At tree-level $f_{2,4}^V = 0$. The form factor f_2^V receives corrections of order α_s/π at loop-level, while f_4^V remains zero through 2-loops. Gauge invariance will also lead to new four-point interactions involving two gauge bosons and the top-quark. In most cases gauge invariance will relate any of the trilinear $t\bar{t}\gamma/Z$ anomalous couplings to others involving the $t\bar{t}W$ vertex. However, Escribano and Masso⁴ have shown that in general all of the anomalous three-point couplings involving the neutral gauge bosons can be unrelated, even when the underlying operators are SM gauge invariant. Of course, within any particular new physics scenario the anomalous couplings will no longer be independent. We note that $f_{2,4}$ take the form of dipole moment type couplings, with the magnetic dipole term f_2 being CP conserving and f_4 , the electric dipole moment term, violating CP. These two form factors are also commonly denoted as κ_V and $\tilde{\kappa}_V$ in the literature.

A generalization of new physics effects on these form factors can be written as

$$f_{1,3} \sim f_{1,3}^{SM} \left(1 + \frac{q^2}{\Lambda^2} \right), \quad f_{2,4} \sim \frac{m_t^2}{\Lambda^2}, \quad (3)$$

where Λ represents the scale of the new interactions. The importance of the large top mass is clear in this parameterization. The γ and Z dipole moment form factors have been explicitly calculated in supersymmetry,⁵ where they are found to take on values typically of order a few $\times 10^{-4}$ for q^2 values near $4M^2$ with M being the supersymmetric mass scale. The one-loop corrections to the chromomagnetic dipole form factors have recently been evaluated⁶ to be $-0.004 \leq f_2^g \leq -0.001$ in the SM and $-0.001 \leq f_2^g \leq -0.01$ in Supersymmetry.

2. Indirect Constraints

Anomalous couplings of the top-quark to on-shell photons and gluons would modify the rate for $B \rightarrow X_s \gamma$. The presence of the magnetic and/or electric dipole moment terms in Eq. (1) would affect the Wilson coefficients of the dipole operators which mediate $b \rightarrow s$ transitions by

$$C_{7,8}(M_W) = C_{7,8}^{SM}(M_W) + \kappa_{\gamma,g} F_{17,8}(m_t^2/M_W^2) + \tilde{\kappa}_{\gamma,g} F_{27,8}(m_t^2/M_W^2). \quad (4)$$

$C_{7,8}^{SM}$ are the SM forms of the one-loop matching conditions for the magnetic and chromomagnetic dipole operators $\mathcal{O}_{7,8}$. We remind the reader that the decay $B \rightarrow X_s \gamma$ is mediated by the magnetic dipole operator \mathcal{O}_7 , however \mathcal{O}_8 also contributes indirectly via operator mixing. The functions $F_{1,2}$ can be found in Ref. 7. Comparing the resulting branching fraction to the CLEO measurement⁸ of the inclusive rate yields the bounds in Fig. 1. In this figure, the allowed region is given by the area inside the solid (dashed) semi-circle when $\kappa_g, \tilde{\kappa}_g = 0$ ($= \kappa_\gamma, \tilde{\kappa}_\gamma$).

Similar indirect constraints⁹ can be found for $t\bar{t}Z$ couplings from the reaction $Z \rightarrow b\bar{b}$.

3. Direct Probes at Colliders

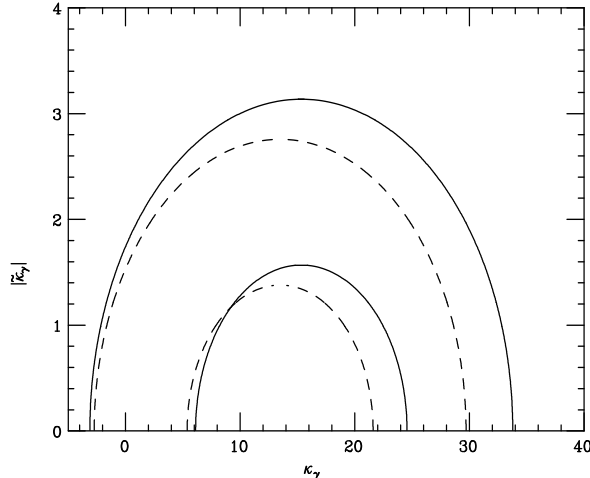


Fig. 1. Constraints on anomalous top-quark photon couplings from $B \rightarrow X_s \gamma$, assuming $m_t(m_t) = 170$ GeV. The solid and dashed curves correspond to the cases described in the text. The allowed regions lie inside the semi-circles.

The direct production of top-quarks at high energy colliders provides the best opportunity to probe these effective couplings. It has been shown¹⁰ that non-standard $t\bar{t}g$ couplings can lead to significant modifications in the characteristics of top pair production at hadron colliders. Since $t\bar{t}$ production at the Tevatron is dominated by the invariant mass region near threshold, there is little effect on the shape of the kinematic distributions from these couplings, whereas the total cross section can deviate substantially from SM expectations. Current cross section measurements¹ hence constrain the chromomagnetic dipole moment to $|f_2^g| \lesssim 0.15 - 0.20$. The larger partonic center of mass energies at the LHC allow access beyond the threshold region and hence yield much higher sensitivity to these couplings via the p_t and pair invariant mass ($M_{t\bar{t}}$) distributions. The analysis of Rizzo¹¹ demonstrates that chromomagnetic dipole moments of order $|f_2^g| \simeq 0.06$ can be probed at the LHC.

Anomalous chromomagnetic dipole moments can also be probed in e^+e^- collisions by studying gluon emission in top pair production. In fact, the presence of such couplings significantly modify the gluon energy distribution in $e^+e^- \rightarrow t\bar{t}g$. A two parameter fit to a Monte Carlo generated data sample for the gluon energy spectrum has been performed in Ref. 12, where a judiciously chosen cut on the minimum gluon jet energy E_g^{min} has been imposed. This cut is necessary to identify the event as $t\bar{t}g$ and avoid the infra-red singularities as well as avoiding contamination from the additional gluon radiation off of the b-quarks in the final state. The resulting 95% C.L. search region in the chromomagnetic - chromoelectric ($f_2^g - f_4^g$)

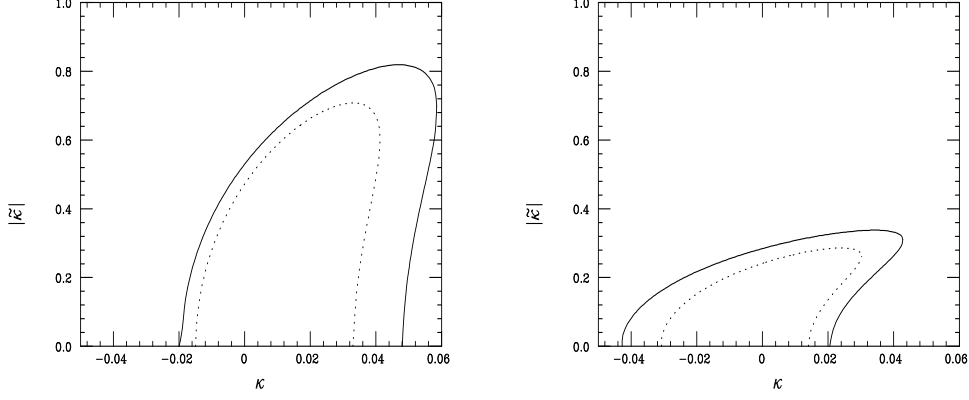


Fig. 2. 95% C.L. allowed region in the $f_4^g - f_2^g$ plane (denoted here as $\tilde{\kappa} - \kappa$) from Ref. 12. The left figure employs $E_g^{min} = 25$ GeV at a 500 GeV NLC with a 50 (solid) or 100 (dotted) fb^{-1} data sample, while the right figure uses employs $E_g^{min} = 50$ GeV at $\sqrt{s} = 1$ TeV with 100 (solid) or 200 (dotted) fb^{-1} .

moment plane is displayed in Fig. 2 for the cuts and luminosities as indicated. We see that the obtainable bounds on f_2^g are comparable to those of the LHC.

Of course, the presence of non-standard $t\bar{t}\gamma/Z$ couplings at the top pair production vertex can also modify the shape of the gluon energy spectrum in $e^+e^- \rightarrow t\bar{t}g$. Following the same Monte Carlo procedure as above¹² the 95% C.L. regions are obtained, taking, for simplicity, only two of the couplings to be simultaneously non-vanishing. The results are presented in Fig. 3 in the $f_2^\gamma - f_4^\gamma$ and $f_2^Z - f_4^Z$ planes. We see that the obtainable constraints on the $t\bar{t}\gamma$ couplings are qualitatively stronger than those for $t\bar{t}Z$.

In a full analysis at the NLC one also needs to fold in the interplay between the possible form factors in both top-quark production and decay. For the top-quark decay, we can write the tbW three point function as

$$\mathcal{L} = \frac{g}{\sqrt{2}} \bar{t} \left[\gamma_\mu (P_L f_{1L}^W + P_R f_{1R}^W) + \frac{ig\sigma_{\mu\nu}q^\nu}{2\sqrt{2}m_t} (P_L f_{2L}^W + P_R f_{2R}^W) \right] bW^\mu + h.c., \quad (5)$$

where $P_{L,R}$ are the helicity projection operators. In the SM, $f_{1L}^W = 1$ and remaining form factors vanish. In the analysis of Ref. 13, all relevant observables for the process $e^+e^- \rightarrow t\bar{t}$ are combined in a likelihood function, using a Monte Carlo generator which includes the helicity information for $t\bar{t}(g)$ production calculated to $\mathcal{O}(\alpha_s)$. An essential ingredient for this analysis is the fact that top-quark pairs are produced in an approximately unique spin configuration in polarized e^+e^- collisions.¹⁴ The resulting simultaneous bounds on non-standard top couplings are given in Table 1 for 10 fb^{-1} at $\sqrt{s} = 500$ GeV with both unpolarized and 80% left-polarized electron beams. We see that the overall sensitivity to possible deviations in these couplings is at the 10 – 15% level. This would correspond, for example, to a $t\bar{t}Z$ electric dipole moment of 8×10^{-18} e-cm.

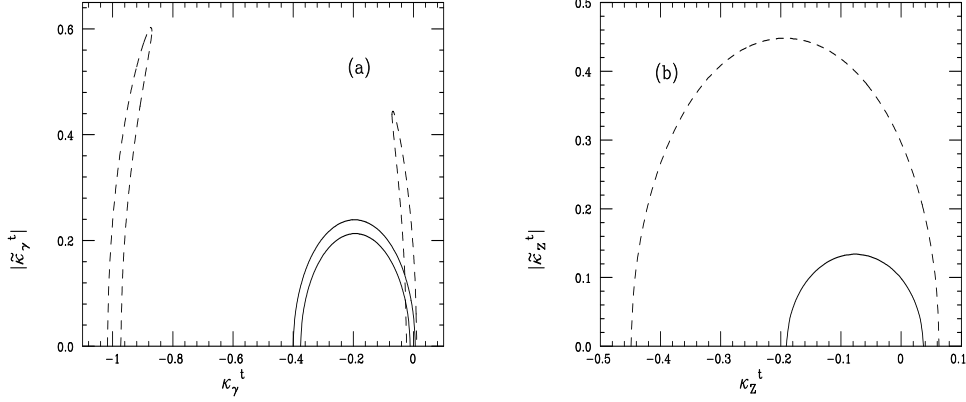


Fig. 3. 95% C.L. allowed regions in the $f_4^\gamma - f_2^\gamma$ and $f_4^Z - f_2^Z$ planes (denoted here as $\tilde{\kappa}_{\gamma,Z} - \kappa_{\gamma,Z}$) from Ref. 12. The allowed regions lie inside the dashed (solid) curves for a 500 (1000) GeV NLC assuming 50 (100) fb^{-1} .

Table 1. Results from the global top-quark form factor analysis of Ref. 13 with a 10 fb^{-1} data sample at a 500 GeV NLC.

Form Factor	SM Value Lowest Order	Limit 68% C.L.	Limit 68% C.L.
$f_{1R}^W(P=0)$	0	± 0.13	± 0.18
$f_{1R}^W(P=80\%)$	0	± 0.06	± 0.10
f_1^Z	v_t	$v_t(1 \pm 0.10)$	$v_t(1 \pm 0.16)$
f_3^Z	a_t	$a_t(1 \pm 0.08)$	$v_t(1 \pm 0.13)$
f_2^γ	0	± 0.07	$^{+0.13}_{-0.11}$
f_4^γ	0	± 0.05	± 0.08
f_2^Z	0	± 0.07	± 0.10
f_4^Z	0	± 0.09	± 0.15
$\mathcal{Im}(f_4^Z)$	0	± 0.06	± 0.09

The possibility of turning the e^+e^- collider into a $\gamma\gamma$ collider via back-scattered laser beams can be exploited to measure the $t\bar{t}\gamma$ couplings independently of the $t\bar{t}Z$ couplings. In this case, the most general form of the differential cross section $d\sigma(\gamma\gamma \rightarrow t\bar{t})/d\cos\theta$ for the $t\bar{t}\gamma$ couplings in Eq. (1) has been computed in Ref. 15. The deviations in the total cross section as a function of the new physics scale Λ are presented in Fig. 4 for the cases (i) $\delta f_1 = s/\Lambda^2, f_2 = m_t^2/\Lambda^2$, (ii) $\delta f_1 = s/\Lambda^2, f_2 = 0$, (iii) $\delta f_1 = 0, f_2 = m_t^2/\Lambda^2$, where δf_1 represents the shift from its SM value. Here, a fixed $\gamma\gamma$ c.m. energy of $\sqrt{s_{\gamma\gamma}} = 400$ GeV is assumed. Note that the effects of the non-standard couplings are found to be slightly more pronounced than in the $e^+e^- \rightarrow t\bar{t}$ production.¹⁵ Measurements of the total cross section alone with an accuracy of 2% could probe new interaction scales up to 10 TeV. In order to compare the $\gamma\gamma$ reach with the results in Table 1 we note that with the above

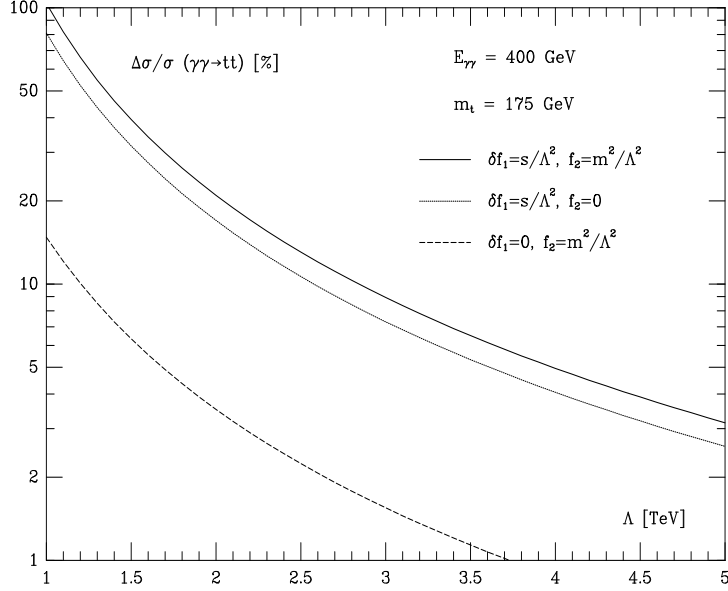


Fig. 4. Percentage change of the total cross section $\gamma\gamma \rightarrow t\bar{t}$ from its SM value for the various form factors as labeled, taking $\sqrt{s_{\gamma\gamma}} = 400$ GeV.

normalization taking $\Lambda = 2.5(5.0)$ TeV, corresponds to $\delta f_1 = \pm 0.025(0.006)$ and $f_2 = \pm 0.005(0.001)$.

4. Exploring CP Violation with γ Beams

The potential to polarize the Compton backscattered photon beam gives rise to interesting ways of studying CP violating effects in $\gamma\gamma \rightarrow t\bar{t}$. The luminosity distributions of the backscattered photons for various helicity combinations of the laser beam and initial electron beam display the following properties:¹⁶ in the case of $\lambda_e \lambda_\gamma = -1$, the luminosity peaks at higher values of invariant mass with a maximum at roughly $W_{\gamma\gamma}/E_{ee} = 80\%$, while for $\lambda_e \lambda_\gamma = +1$ the spectrum is almost Gaussian like (for low values of the intrinsic photon spread), peaking at lower energies. These characteristics allow the measurement of various CP-odd correlations. For example, CP-odd asymmetries can be formed when the two $J = 0$ amplitudes

$$\begin{aligned} \mathcal{A}[\gamma\gamma \rightarrow X(CP = +1)] &\sim \vec{\epsilon}_1 \cdot \vec{\epsilon}_2, \\ \mathcal{A}[\gamma\gamma \rightarrow X(CP = -1)] &\sim (\vec{\epsilon}_1 \times \vec{\epsilon}_2) \cdot \vec{k}, \end{aligned} \quad (6)$$

are non-vanishing, with $\vec{\epsilon}_{1,2}$ being the polarization of the two photon beams and \vec{k} the momentum carried by one of the photons in the $\gamma\gamma$ c.m. frame. Here, X represents a non-CP eigenstate, such as, $t\bar{t}$ in the case of non-vanishing $t\bar{t}\gamma$ electric dipole moments, or X can correspond to a Higgs boson with CP violating couplings in multi-Higgs models. The first example has been studied in Refs. 17,18,19.

Table 2. 90% C.L. bounds on $\mathcal{Im} f_4^\gamma$ in units of 10^{-16} e-cm, for $m_t = 174$ GeV, electron beam energy of 250 GeV, and 20 fb^{-1} . From Ref. 19.

λ_e^1	λ_e^2	λ_γ^1	λ_γ^2	$\mathcal{Im} f_4^\gamma$ (10^{-16} e-cm)
-0.5	-0.5	-1	-1	2.76
-0.5	-0.5	1	-1	0.23
-0.5	-0.5	1	1	0.54
0.5	-0.5	-1	-1	2.31
0.5	-0.5	1	-1	1.03
0.5	-0.5	1	1	1.12
Unpolarized				1.19

Choi and Hagiwara¹⁷ have investigated a polarization asymmetry which isolates the electric dipole moment contribution by taking the difference of $t\bar{t}$ event rates at $\chi = +\pi/4$ and $\chi = -\pi/4$, where χ is the angle between the directions of maximum linear polarization of the two laser beams in the e^+e^- (or e^-e^-) c.m. frame. For $\sqrt{s} = 500$ GeV with 20 fb^{-1} , they find that this asymmetry can probe top electric dipole moments down to $e|\mathcal{Re} f_4^\gamma|/2m_t < 1.16 \times 10^{-17}$ e-cm for $m_t = 170$ GeV. Baek *et al.*,¹⁸ perform a similar analysis and find $|\mathcal{Re} f_4^\gamma| < 0.16$, for the same machine parameters. Note that these results are comparable to the potential constraints listed in Table 1 obtained from top decay spin correlation analyses in $e^+e^- \rightarrow t\bar{t}$. Poulse and Rindani¹⁹ have obtained similar results by examining the charge and combined charge and forward-backward asymmetries. Folding in the full photon energy and luminosity distributions they obtain the 90% C.L. bounds on $\mathcal{Im} f_4^\gamma$ shown in Table 2 for various helicity combinations as listed and for electron beam energies of 250 GeV. These limits are shown to improve by an order of magnitude for 500 GeV electron beams.

CP violation studies in $\gamma\gamma \rightarrow H \rightarrow t\bar{t}$ with unpolarized beams have been performed in Ref. 20, using triple-product correlations and a variety of polarization asymmetries in top semi-leptonic decays. These authors examine the case of two-Higgs-doublet models which contain explicit CP violation in both the Yukawa couplings and in the Higgs potential. A typical result is given by the longitudinal polarization asymmetry defined by $\hat{\mathbf{k}} \cdot (\mathbf{s}_+ - \mathbf{s}_-)$, where \mathbf{k} is the momentum of the t -quark and $\mathbf{s}_+, \mathbf{s}_-$ are the spin operators of t and \bar{t} , respectively. This observable is displayed in Fig. 5 as a function of the $\gamma\gamma$ c.m. energy, where the mass of the lightest neutral Higgs boson is taken to be 400 GeV, the ratio of vacuum expectation values of the two doublets is $\tan \beta \equiv v_2/v_1 = 1$, and $m_t = 175$ GeV. We see that the asymmetry grows large near the resonance region. The other observables discussed in this reference display similar characteristics and could provide a window into the CP properties of extended Higgs sectors.

5. Flavor Changing Top Couplings

Another interesting possibility is to study the flavor changing top-quark vertices

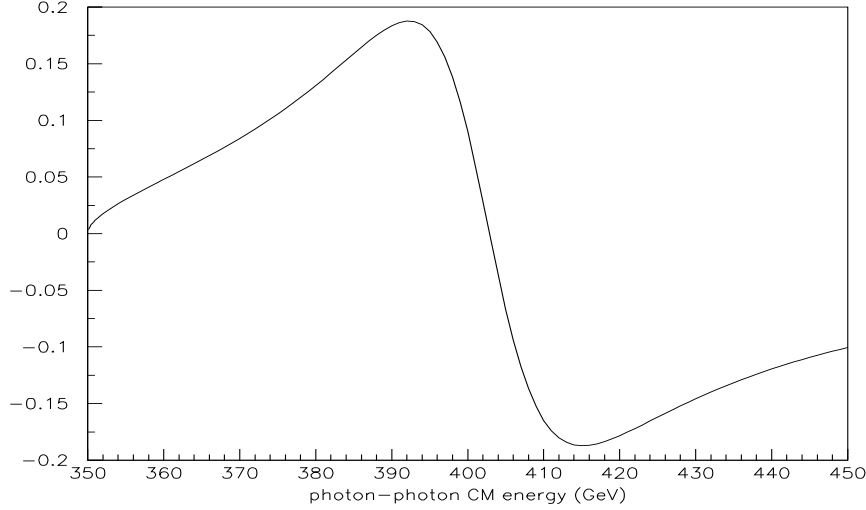


Fig. 2

Fig. 5. Longitudinal polarization asymmetry described in the text as a function of the $\gamma\gamma$ c.m. energy.

$tq\gamma/Z$ where $q = c$ or u at lepton and photon colliders. The expectations in the SM (and simple extensions thereof, such as supersymmetry)²¹ for these couplings are too small to be observed and thus any experimental evidence for their existence implies new interactions. Here, we consider only the lowest dimension CP-conserving operators in the effective Lagrangian involving the anomalous top-quark couplings,

$$\mathcal{L}^{eff} = \frac{e}{\Lambda} \kappa_\gamma \bar{t} \sigma_{\mu\nu} c F^{\mu\nu} + \frac{g}{2c_w} \bar{t} \left[g_{ZL} \gamma_\mu P_L + g_{ZR} \gamma_\mu P_R + \frac{i\sigma_{\mu\nu} q^\nu}{m_t} \kappa_Z \right] q Z^\mu + h.c., \quad (7)$$

where Λ is the cutoff of the effective theory, and $P_{L,R}$ are the usual helicity projection operators. CDF has placed the 95% C.L. bounds on the flavor changing neutral current (FCNC) decays of the top-quark of $B(t \rightarrow cZ + uZ) < 33\%$ and $B(t \rightarrow c\gamma + u\gamma) < 2.9\%$. The latter limit implies $\kappa_\gamma/\Lambda < 0.73/\text{TeV}$. An extensive analysis²³ has shown that the LHC can improve on these constraints by directly searching for the FCNC decays and probe the pertinent anomalous couplings to the level of $\kappa_\gamma/\Lambda \simeq 0.01/\text{TeV}$ and $g_{tc} = \sqrt{g_{ZL}^2 + g_{ZR}^2} \simeq 0.02$ which corresponds to a branching fraction of $B(t \rightarrow qZ) < 2 \times 10^{-4}$.

The NLC can probe these couplings in the direct production vertex via the reaction $e^+e^- \rightarrow t\bar{c} + \bar{t}c$. In this case, the cross sections are found²⁴ to be large and the signature clean with a single hard jet in one hemisphere and a top-quark decaying to $bW \rightarrow b\ell\nu_\ell$ in the other. These kinematic characteristics allow for a clear separation of the signal from the WW pair background by imposing a set of idealized cuts. Figure 6 displays the resulting 95% C.L. bounds obtainable on κ_Z from this analysis, with and without imposing a 50% b-tagging identification efficiency, as a function of luminosity for $\sqrt{s} = 500$ GeV. The expectations for constraints on κ_γ are comparable to those above for the LHC, *i.e.*, $\kappa_\gamma/\Lambda \simeq 0.01/\text{TeV}$.

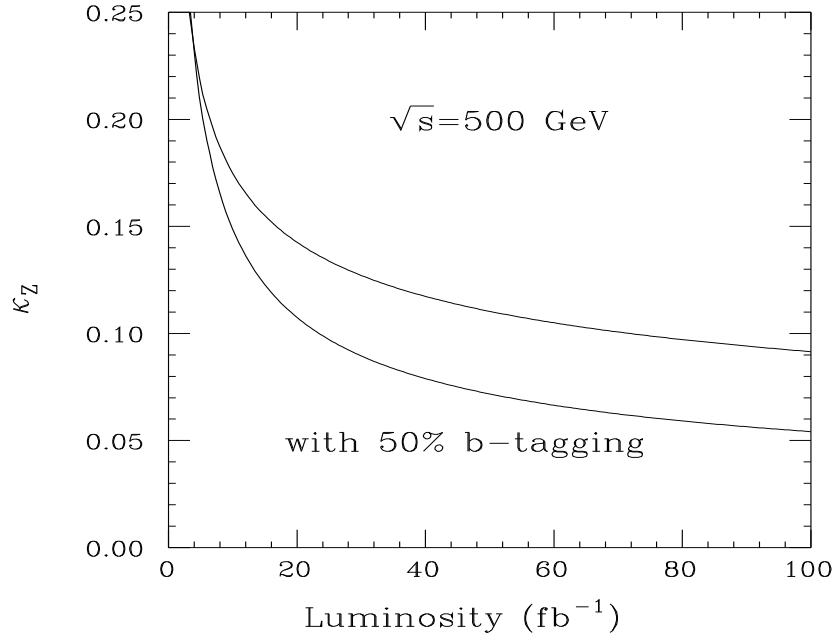


Fig. 6. Expected 95% C.L. bounds on κ_Z as a function of luminosity at a 500 GeV NLC, with and without a 50% b-tagging identification efficiency as indicated.

The radiative flavor changing couplings can also be tested at a $\gamma\gamma$ collider via $t\bar{q} + \bar{t}q$. This has been investigated in Ref. 25, with the result

$$\sigma(\gamma\gamma \rightarrow t\bar{c} + \bar{t}c \rightarrow b\ell^+\nu\bar{c} + \bar{b}\ell^-\bar{\nu}c) = \left[\frac{\kappa_\gamma/\Lambda}{0.16/\text{TeV}} \right]^2 76.4 \text{ fb}. \quad (8)$$

This corresponds to an expected search reach of $\kappa_\gamma/\Lambda < (0.05/\text{TeV})/\sqrt{\mathcal{L}/10 \text{ fb}^{-1}}$ for a fixed $\gamma\gamma$ c.m. energy of 400 GeV.

6. Summary

We have presented an overview of the ability of lepton and photon colliders to probe CP conserving and violating anomalous couplings of the top-quark. In particular, some advantages of a $\gamma\gamma$ collider over the e^+e^- case is that the $t\bar{t}\gamma$ three-point function can be isolated from that for $t\bar{t}Z$, the $t\bar{t}$ production cross section is larger, and the potential for linear photon polarization provides some simple probes of CP violation. When comparisons can be made, we see that both types of machines can yield comparable, if not better, constraints than those obtainable in hadronic collisions.

References

1. B. Klima, talk given at the *12th Les Rencontres de Physique de la Vallée d'Aoste: Results and Perspectives in Particle Physics*, La Thuile, Italy, March 1998.
2. The LEP Collaborations, the LEP Electroweak Working Group, and the SLD Heavy Flavor Group, CERN-PPE/97-154 (1997).
3. For a list of references, see, J.L. Hewett, T. Takeuchi, and S. Thomas in *Electroweak Symmetry Breaking and New Physics at the TeV Scale*, ed. T. Barklow *et al.*, (World Scientific, Singapore 1996), hep-ph/9603391.
4. R. Escrivano and E. Masso, Phys. Lett. **B301**, 419 (1993), and Nucl. Phys. **B429**, 19 (1994).
5. A. Bartl, *et al.*, Nucl. Phys. **B507**, 35 (1997).
6. R. Martinez *et al.*, hep-ph/9709478.
7. J.L. Hewett and T.G. Rizzo, Phys. Rev. **D49**, 319 (1994).
8. M.S. Alam *et al.*, CLEO Collaboration, Phys. Rev. Lett. **74**, 2885 (1995).
9. S. Dawson and G. Valencia, Phys. Rev. **D53**, 1721 (1996).
10. D. Atwood, A. Kagan, and T.G. Rizzo, Phys. Rev. **D52**, 6264 (1995); T.G. Rizzo, Phys. Rev. **D53**, 6218 (1996); K. Cheung, Phys. Rev. **D53**, 3604 (1996); P. Haberl, O. Nachtmann, and A. Wilch, Phys. Rev. **D53**, 4875 (1996).
11. T.G. Rizzo in *New Directions for High-Energy Physics*, Snowmass, CO, 1996, ed. D.G. Cassel, hep-ph/9609311.
12. T.G. Rizzo, Phys. Rev. **D50**, 4478 (1994), and in *New Directions for High-Energy Physics*, Snowmass, CO, 1996, ed. D.G. Cassel, hep-ph/9610373.
13. *Physics and Technology of the Next Linear Collider*, BNL Report BNL 52-502, 1996; R. Frey in *Proceedings of the Workshop on Physics and Experiments with Linear Colliders*, Iwate, Japan, 1995, hep-ph/9606201; C. Schmidt, hep-ph/9504434; C.R. Schmidt, Phys. Rev. **D54**, 3250 (1996.)
14. S. Parke and Y. Shadmi, Phys. Lett. **B387**, 199 (1996).
15. A. Djouadi, in *Proceedings of the Workshop on e^+e^- Collisions at 500 GeV: the Physics Potential*, ed. P. Zerwas, Report DESY-92-123B; A. Djouadi, J. Ng, and T.G. Rizzo, in *Electroweak Symmetry Breaking and New Physics at the TeV Scale*, ed. T. Barklow *et al.*, (World Scientific, Singapore 1996), hep-ph/9504210.
16. See, for example, D. Bauer, Int. J. Mod. Phys. **A11**, 1637 (1996); D.L. Borden in *Proceedings of the Workshop on Physics and Experiments with Linear e^+e^- Colliders*, ed. F.A. Harris *et al.*, (World Scientific, Singapore 1993).
17. S.Y. Choi and K. Hagiwara, Phys. Lett. **B359**, 369 (1995).
18. M.S. Baek *et al.*, Phys. Rev. **D56**, 6835 (1997).
19. P. Poulose and S.D. Rindani, hep-ph/9709225.
20. H. Anlauf, W. Bernreuther, and A. Brandenburg, Phys. Rev. **D52**, 3803 (1995), Erratum **D53**, 1725 (1996).
21. See, for example, G. Eilam, J.L. Hewett, and A. Soni, Phys. Rev. **D44**, 1473 (1991).
22. G. Chiarelli (CDF Collaboration), in *Proceedings of the 32nd Rencontres de Moriond: QCD and High Energy Hadronic Interactions*, Les Arcs, France, March 1997, Fermilab-CONF-97/143-E.
23. T. Han *et al.*, Phys. Rev. **D55**, 7241 (1997); T. Han, R. Peccei, and Z. Zhang, Nucl. Phys. **B454**, 527 (1995).
24. T. Han and J.L. Hewett, in preparation.
25. K.J. Abraham *et al.*, hep-ph/9707476.